Biomedical Optics EXPRESS

Quantitative comparison of optimized nanorods, nanoshells and hollow nanospheres for photothermal therapy

Sameh Kessentini[1,2] **and Dominique Barchiesi**[1,3]

[1]*Project Group for Automatic Mesh Generation and Advanced Methods - Gamma3 Project (UTT-INRIA), University of Technology of Troyes, 12 rue Marie Curie - BP 2060, 10010 Troyes Cedex, France*
[2]*samehkessentini@gmail.com*
[3]*dominique.barchiesi@utt.fr*

Abstract: The purpose of this study is to get more efficient gold nanoparticles, for necrosis of cancer cells, in photothermal therapy. Therefore a numerical maximization of the absorption efficiency of a set of nanoparticles (nanorod, nanoshell and hollow nanosphere) is proposed, assuming that all the absorbed light is converted to heat. Two therapeutic cases (shallow and deep cancer) are considered. The numerical tools used in this study are the full Mie theory, the discrete dipole approximation and the particle swarm optimization. The optimization leads to an improved efficiency of the nanoparticles compared with previous studies. For the shallow cancer therapy, the hollow nanosphere seems to be more efficient than the other nanoparticles, whereas the hollow nanosphere and nanorod, offer comparable absorption efficiencies, for deep cancer therapy. Finally, a study of tolerance for the size parameters to guarantee an absorption efficiency threshold is included.

OCIS codes: (170.0170) Medical optics and biotechnology; (170.1020) Ablation of tissue; (170.5180) Photodynamic therapy; (350.5340) Photothermal effects.

References and links

1. C. Liu, C. C. Mi, and B. Q. Li, "Energy absorption of gold nanoshells in hyperthermia therapy," IEEE Trans. Nanobiosci. **7**(3), 206–214 (2008).
2. X. Huang and M. A. El-Sayed, "Gold nanoparticles optical properties and implementations in cancer diagnosis and photothermal therapy," J. Adv. Res. **1**(1), 13–28 (2010).
3. V. K. Pustovalov, A. S. Smetannikov, and V. P. Zharov, "Photothermal and accompanied phenomena of selective nanophotothermolysis with gold nanoparticles and laser pulses," Laser Phys. Lett. **5**(11), 775–792 (2008).
4. F. A. Duck, *Physical Properties of Tissue: A Comprehensive Reference Book* (Academic, London, 1990).
5. L. R. Hirsch, R. J. Stafford, J. A. Bankson, S. R. Sershen, B. Rivera, R. E. Price, J. D. Hazle, N. J. Halas, and J. L. West, "Nanoshell-mediated near-infrared thermal therapy of tumors under magnetic resonance guidance," Proc. Natl. Acad. Sci. U.S.A. **100**, 13549–13554 (2003).
6. A. M. Schwartzberg and J. Z. Zhang, "Novel optical properties and emerging applications of metal nanostructures," J. Phys. Chem. C **112**, 10323–10337 (2008).
7. A. M. Schwartzberg, T. Y. Olson, C. E. Talley, and J. Z. Zhang, "Synthesis, characterization, and tunable optical properties of hollow gold nanospheres," J. Phys. Chem. B **110,**, 19935–19944 (2006).
8. H. Takahashi, T. Niidome, A. Nariai, Y. Niidome, and S. Yamada, "Gold nanorod-sensitized cell death: microscopic observation of single living cells irradiated by pulsed near-infrared laser light in the presence of gold nanorods," Chem. Lett. **35**, 500–501 (2006).
9. H. Takahashi, T. Niidome, A. Nariai, Y. Niidome, and S. Yamada, "Photothermal reshaping of gold nanorods prevent further cell death," Nanotechnology **17**, 4431–4435 (2006).

#159136 - $15.00 USD Received 29 Nov 2011; revised 25 Jan 2012; accepted 27 Jan 2012; published 22 Feb 2012

10. K. J. Prashant, K. S. Lee, I. H. El-Sayed, and M. A. El-Sayed, "Calculated absorption and scattering properties of gold nanoparticles of different size, shape and composition: application in biological imaging and biomedicine," J. Phys. Chem. B **110**, 7238–7248 (2006).
11. N. Harris, M. J. Ford, P. Mulvaney, and M. B. Cortie, "Tunable infrared absorption by metal nanoparticles: the case of gold rods and shells," Gold Bull. **41**, 5–14 (2008).
12. J. L. Li, D. Day, and M. Gu, "Ultra-low energy threshold for cancer photothermal therapy using transferrin-conjugated gold nanorods," Adv. Mater. **20**, 3866–3871 (2008).
13. T. Grosges, D. Barchiesi, T. Toury, and G. Gréhan, "Design of nanostructures for imaging and biomedical applications by plasmonic optimization," Opt. Lett. **33**, 2812–2814 (2008).
14. C. F. Bohren and D. R. Huffman, *Absorption and Scattering of Light by Small Particles* (Wiley, New York, 1998).
15. S. Kessentini, D. Barchiesi, T. Grosges, and M. L. de la Chapelle, "Particle swarm optimization and evolutionary methods for plasmonic biomedical applications," in *IEEE Congress on Evolutionary Computation (CEC 2011)* (IEEE, 2011), pp. 2315–2320.
16. K. S. Lee and M. A. El-Sayed, "Dependence of the enhanced optical scattering efficiency relative to that of absorption of gold metal nanorods on aspect ratio, size, end-cap shape, and medium refractive," J. Phys. Chem. B **109**, 20331–20338 (2005).
17. B. T. Draine and P. J. Flatau, "Discrete-dipole approximation for periodic targets: theory and tests," J. Opt. Soc. Am. A **25**, 2693–2703 (2008).
18. H. Devoe, "Optical properties of molecular aggregates. I. classical model of electronic absorption and refraction," J. Chem. Phys. **41**, 393–400 (1964).
19. H. Devoe, "Optical properties of molecular aggregates. II. classical theory of the refraction, absorption, and optical activity of solutions and crystals," J. Chem. Phys. **43**, 3199–3208 (1965).
20. E. Purcell and C. R. Pennypacker, "Scattering and absorption of light by nonspherical dielectric grains," Astr. J. **186**, 705 (1973).
21. B. T. Draine and P. J. Flatau, "Discrete-dipole approximation for scattering calculations," J. Opt. Soc. Am. A **11**, 1491–1499 (1994).
22. B. T. Draine and P. J. Flatau, "User guide to the discrete dipole approximation code DDSCAT 7.1," (2010), `http://arXiv.org/abs/1002.1505v1`.
23. S. Kessentini, D. Barchiesi, T. Grosges, L. Giraud-Moreau, and M. L. de la Chapelle, "Adaptive non-uniform particle swarm application to plasmonic design," Int. J. Appl. Metaheuristic Comput. (IJAMC) **2**, 18–28 (2011).
24. D. Barchiesi, "Adaptive non-uniform, hyper-ellitist evolutionary method for the optimization of plasmonic biosensors," in *Proc. Int. Conf. Computers & Industrial Engineering CIE 2009* (2009), pp. 542–547.
25. J. Kennedy and R. Eberhart, "Particle swarm optimization," in *IEEE International Conference on Neural Networks* (IEEE, 1995), vol. IV, pp. 1942–1948.
26. Z.-H. Zhan, J. Zhang, Y. Li, and H. S.-H. Chung, "Adaptive particle swarm optimization," IEEE Trans. Syst. Man Cybern. Part B Cybern. **39**, 1362–1381 (2009).
27. D. H. Wolpert and W. Macready, "No free lunch theorems for optimization," IEEE Trans. Evolut. Comput. **1**, 67–82 (1997).
28. S. Kessentini and D. Barchiesi, "A new strategy to improve particle swarm optimization exploration ability," in *2010 Second WRI Global Congress onIntelligent Systems (GCIS)* (IEEE, 2010), vol. 1, pp. 27 – 30.
29. P. C. Chen, S. C. Mwakwari, and A. K. Oyelere, "Gold nanoparticles: from nanomedicine to nanosensing," Nanotechnol. Sci. Appl. **1**, 45–66 (2008).
30. C. R. Patra, R. Bhattacharya, D. Mukhopadhyay, and P. Mukherjee, "Fabrication of gold nanoparticles for targeted therapy in pancreatic cancer," Adv. Drug Delivery Rev. **62**, 346–361 (2010).
31. D. Pissuwan, S. M. Valenzuel, and M. B. Cortie, "Prospects for gold nanorod particles in diagnostic and therapeutic applications," Biotechnol. Genetic Eng. Rev. **25**, 93–112 (2008).
32. C. Ungureanu, R. G. Rayavarapu, S. Manohar, and T. V. Leeuwen, "Discrete dipole approximation simulations of gold nanorod optical properties: Choice of input parameters and comparison with experiment," J. Appl. Phys. **105**, 102032–102039 (2009).
33. D. Barchiesi, D. S. Kessentini, and T. Grosges, "Sensitivity analysis for designing active particles in photothermal cancer therapy," in *Advances in Safety, Reliability and Risk Management*, C. Bérenguer and A. Grall, eds. (Taylor & Francis, London, 2011), pp. 2197–2204.
34. T. Grosges, D. Barchiesi, S. Kessentini, G. Gréhan, and M. Lamy de la Chapelle, "Nanoshells for photothermal therapy: a Monte-Carlo based numerical study of their design tolerance," Biomed. Opt. Express **2**(6), 1584–1596 (2011).
35. V. V. Tuchin, *Tissue optics: Light Scattering Methods and Instruments for Medical Diagnosis* (SPIE, Bellingham, Washington, 2007).
36. J. Vera and Y. Bayazitoglu, "A note on laser penetration in nanoshell deposited tissue," Int. J. Heat Mass Transfer **52**, 3402–3406 (2009).
37. J. Z. Zhang, "Biomedical application of shape-controlled plasmonic nanostructure: a case study of hollow gold nanospheres for photothermal ablation therapy of cancer," J. Phys. Chem. Lett. **1**, 686–695 (2010).
38. T. Qiu, W. Zhang, and P. K. Chu, "Recent progress in fabrication of anisotropic nanostructures for surface-

#159136 - $15.00 USD Received 29 Nov 2011; revised 25 Jan 2012; accepted 27 Jan 2012; published 22 Feb 2012

enhanced raman spectroscopy," Recent Patents Nanotechnol. **3**, 10–20 (2009).
39. F. Ratto, P. Matteini, F. Rossi, and R. Pini, "Size and shape control in the overgrowth of gold nanorods," J. Nanoparticle Res. **12**, 2029-2036 (2010).

1. Introduction

Photothermal therapy (PTT) is based on the interaction of a suitable light source with gold nanoparticles embedded in cells, which produces a sufficient elevation of temperature to induce their necrosis. The predominating benefits of such treatment are both safety and efficiency as PTT limits the possible damage of healthy cells (unlike microwave ablation, magnetic thermal ablation, and focused ultrasound therapy) [1]. Moreover, the gold nanoparticles, which are biocompatible and nontoxic, can be easily conjugated to antibodies. Hence, once injected into the body, they get fixed on the cancer cells as represented in Fig. 1(a). Then under suitable illumination they absorb a large amount of light (Fig. 1(b)). Almost all the absorbed light is converted to heat via a series of nonradiative processes [2]. Therefore the cancer cells containing gold nanoparticles receive sufficient heat to induce their necrosis [3] with minimal damage to their surrounding (localized heat delivery).

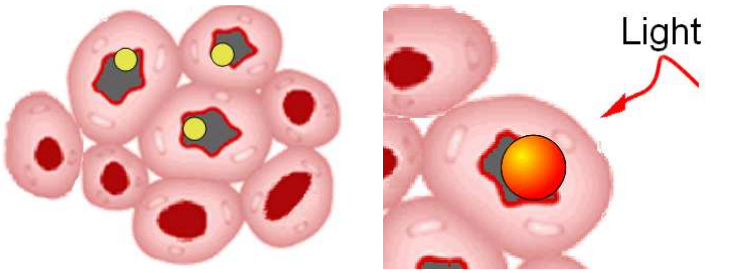

(a) Nanoparticles fixed to cancer cells (b) Absorption of light by nanoparticles

Fig. 1. Photothermal therapy using gold nanoparticles.

The choice of the illumination conditions is dictated by the therapeutic application. Two optical windows exist in tissue, as it is mainly transparent within these regions of wavelengths. The main one lies between 600 and 1300 nanometers (nm) and a second one from 1600 to 1850 nm [4]. In these windows, the gold nanoparticles absorb the light millions of times more than the organic molecules [1]. PTT in the visible region is suitable for shallow cancer (e.g. skin cancer). Whereas for in vivo therapy of tumors deeply seated under skin, Near Infra Red (NIR) light is required because of its deep penetration. In fact, the hemoglobin and water molecules in tissue have minimal absorption and a limited attenuation of scattering in this spectral region. Both the visible (VIS) and NIR regions are therefore investigated (the wavelengths of 633 nm and 800 nm are considered).

The purpose of this study is to compare the efficiencies of nanoparticles for photothermal therapy. Their therapeutic efficiency depends not only on their shape but also on their size. The shape of the gold nanoparticles, commonly used for PTT, are spheres, shells (with silica core), hollow spheres and rods.

In 2003, Hirsch et al. [5] demonstrated the NIR PTT, both in vitro and in vivo, using gold nanoshells. While in the visible range, nanospheres are of interest only for skin cancer [2]. The advantages of spherical shape were demonstrated. In fact, the non spherical nanostructures can exhibit a broad spectrum absorption. A plasmon tunability and a narrow absorption band are preferred to get a better coupling with the illumination [6]. Hollow nanospheres and nanoshells

#159136 - $15.00 USD Received 29 Nov 2011; revised 25 Jan 2012; accepted 27 Jan 2012; published 22 Feb 2012

can guarantee such tunable behavior at different wavelengths ranging from VIS to NIR, by adjusting their size parameters [7]. Nevertheless, hollow nanospheres are synthesized with great precision and controlled dimensions [7] whereas, forming a uniform shell on the silica core remains challenging [2].

Some advantages of nanorods are reported in Ref. [2]. For instance, using nanorods illuminated by pulsed laser source, the destruction of a single cell can be achieved (selectivity improvement), the nanorods being reshaped into nanospheres (in situ) [8, 9]. This degradation of the nanorod prevents further death of cell [8] (as nanospheres have very limited absorption in NIR). Moreover, in most comparative studies, the nanorods were shown to be more efficient than the nanoshells and therefore require lower laser intensity for photothermal therapy [2]. However these studies [10, 11] covered some samples of nanoshells, which had not been optimized (the absorption efficiency Q_{abs} is restricted to 18 whereas it could achieve 30 using Ag nanoshells). In these comparisons, the incoming light is assumed to be linearly polarized along the nanorod longitudinal axis, whereas in therapeutic applications the nanorods are randomly oriented. This random orientation prevents to achieve the maximum absorption efficiency. To enhance the treatment efficiency, a circular polarization is used to activate as many nanorods as possible [12]. Therefore both the circular polarization and the linear polarization are considered in this study. We propose to find the size parameters that enable the maximum absorption efficiency for each type of nanoparticle, and to compare them (only few previous studies were devoted to the numerical optimization of nanoshells [13]).

Consequently the target is to maximize the absorption efficiency for nanoshell, hollow nanosphere and nanorod in two therapeutic cases: the treatment of shallow cancer under VIS irradiation and of deep cancer under NIR irradiation. For this, numerical methods are required to compute the absorption efficiency Q_{abs} for different shapes. To compute Q_{abs}, we use the Mie theory for nanoshells and hollow nanospheres [14], and the discrete dipole approximation (DDA) for nanorods. Moreover, an optimization algorithm must be used to maximize it. A specific particle swarm optimization (PSO) algorithm is chosen, based on the results of the comparison between different methods of optimization for plasmonic applications [15].

The paper is organized as follows: in the second section, the numerical methods used to compute the absorption efficiency and the optimization algorithm are described. In the third section, the different therapeutical cases and the assumptions for simulations are presented, before carrying comparisons and computing the tolerance for the geometrical parameters of the nanoparticles. Finally, concluding remarks are given in the fourth section.

2. Numerical and optimization tools

In this section brief overviews of the numerical methods used to compute the absorption efficiency Q_{abs} and the optimization algorithm are presented. The numerical methods used to compute Q_{abs} are the full Mie theory for nanoshells and hollow nanospheres (as they present spherical symmetry) and the discrete dipole approximation (DDA) for nanorods. Then, Q_{abs} can be maximized using an adequate optimization algorithm [15] which is the adaptive particle swarm optimization (APSO).

2.1. Absorption efficiency for spherical nanoparticle

The computation of the absorption efficiency Q_{abs} could be achieved analytically for spherical shapes (hollow nanosphere and nanoshell). This analytical solution is derived by solving the scalar Helmholtz equation using separation of variables in spherical coordinate system [14]. Then, the electromagnetic fields are expanded using the spherical vectors (solutions of the vector Helmholtz equation). The coefficients of the expansion are determined by fitting the boundary conditions and the radiation condition. For spherical nanoparticle, the absorption efficiency

#159136 - $15.00 USD Received 29 Nov 2011; revised 25 Jan 2012; accepted 27 Jan 2012; published 22 Feb 2012

Q_{abs} is related to the absorption cross section C_{abs} and is given by

$$Q_{abs} = \frac{C_{abs}}{\pi r_2^2} = \frac{2}{y^2} \sum_{n=1}^{\infty} \left[(2n+1) \left\{ \left(\Re(a_n + b_n) - (|a_n|^2 + |b_n|^2) \right) \right\} \right], \quad (1)$$

where a_n and b_n are two of the coefficients associated to the expansion of fields. They are complex functions depending on the size variables: $x = kr_1$, $y = k(r_1 + e)$, with r_1 the inner radius, $e = r_2 - r_1$ the shell thickness (Fig. 2), $k = 2\pi/\lambda$, and λ the wavelength of the monochromatic illumination (equations and further details could be found in [14]).

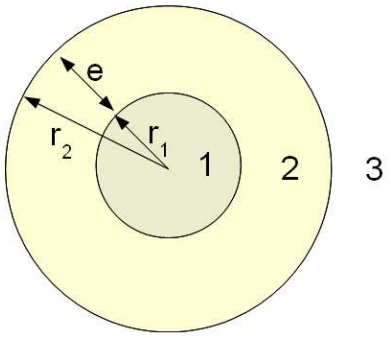

Fig. 2. Spherical nanoparticle: nanoshell or hollow nanosphere (inner radius r_1, outer radius r_2 and shell thickness $e = r_2 - r_1$)

2.2. The discrete dipole approximation (DDA)

When the analytical solution of Maxwell's equations is unknown, it is necessary to use numerical methods. Several numerical methods were introduced such as the DDA, the method of moments, the finite difference time domain method and the finite element method. Each of these methods presents some advantages and drawbacks. However the DDA is widely used for absorption and scattering calculations by nanoparticles used in PTT, the computing time (main drawback of DDA) remaining short for small size targets. Moreover, the accuracy of the method was checked by comparison to analytical solutions for spherical nanoparticle [16], ellipsoid [16] and infinite cylinder [17]. Therefore we use the DDA in this study, for non-spherical particles. In what follows, a brief description of this method and of the numerical tool are given.

The method was firstly developed by Devoe [18, 19], and Purcell and Pennypacker [20]. The main idea is to discretize the geometry of the naoparticle into a set of N elements ($j = 1..N$) with polarizabilities α_j, located at $\mathbf{r}_j$. Each dipole has a polarization $\mathbf{P}_j = \alpha_j \mathbf{E}_j$, where $\mathbf{E}_j$ is the electric field at $\mathbf{r}_j$ induced by the incident wave and the sum of the dielectric fields induced by interaction with other dipoles. A system of $3N$ complex linear equations (see [21] for details) must be solved to find polarizations $\mathbf{P}_j$ and evaluate the absorption cross section following:

$$C_{abs} = \frac{4\pi k}{|\mathbf{E}_0|^2} \sum_{j=1}^{N} \left\{ Im \left[\mathbf{P}_j . (\alpha_j^{-1})^* \mathbf{P}_j^* \right] - \frac{2}{3} k^3 |\mathbf{P}_j|^2 \right\}. \quad (2)$$

The Fortran code DDSCAT 7.1, developed by Draine and Flatau, is used for calculating scattering and absorption of light by irregular particles based on the DDA [22]. DDSCAT enables to deal with many shapes such as cylinder, ellipsoid or cylinder with capped ends. It also offers

#159136 - $15.00 USD Received 29 Nov 2011; revised 25 Jan 2012; accepted 27 Jan 2012; published 22 Feb 2012

the possibility of editing new shapes. We edit some shapes to ensure flexible orientation of the nanoparticle relative to the incident polarization of light. Then the inter-dipole distance should be chosen. For this, the DDA results are compared to those of Mie theory for a sphere of radius 40 nm. The results are reported in Fig. 3 and show that an inter-dipole distance d equal to 1 nm is sufficient to achieve reasonable accuracy in this size range.

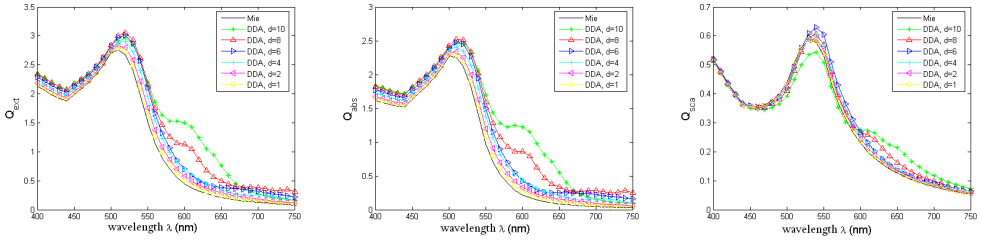

(a) Extinction efficiency (b) Absorption efficiency (c) Scattering efficiency

Fig. 3. Comparison of DDA with Mie theory for different values of the inter-dipole distance d for a sphere of radius 40 nm.

2.3. *The optimization algorithm: the adaptive PSO*

The optimization goal is to maximize the fitness function Q_{abs} within a search space of the size parameters. The computing time of Q_{abs} using the DDA can sometimes exceed half an hour for a unique wavelength depending on some parameters: the size of the target, the discretization used, the error tolerance, the optical index, and the performance of the computer. Therefore a deterministic sweep of the search space may be prohibitive, and an adequate optimization algorithm must be used.

A comparison of four optimization algorithms [23, 24, 25, 26] reveals different performances depending on the problem [15]. Nevertheless, they are faster than the systematic study through simple loops on the size parameters. Based on the "no free lunch" theorems [27], showing that learning algorithms cannot be universally good and that any elevated performance over one class of problems is exactly paid for in performance over another class, we need to ensure the efficiency of algorithms on plasmonic biomedical applications. Therefore a benchmark was introduced: the cases of plane biosensors, and of the absorption within the shell of hollow nanospheres [15]. These problems were shown to be multimodal in addition to have various topologies. Therefore the optimization algorithm must converge rapidly to the global optimum solution, avoiding the local optima.

As suggested in [15], we use the adaptive PSO [26] to which some improvements were added [28]. Let us introduce firstly the standard PSO proposed by Kennedy and Eberhart in 1995 [25]. The PSO mimics the behavior of a swarm of bees in search of pollen. In this algorithm, vectors of decision variables x (in this case, the size parameters) are randomly generated at the beginning of the algorithm. These vectors are considered as the positions of bees (or particles) of a swarm. We should note the difference between the nanoparticles used in PTT and the "particle" used in PSO to denote a vector of decision variables $x(t)$. The particles communicate good positions to each other and adjust their own position $x(t)$ and velocity $V(t)$ following:

$$V(t+1) = \omega V(t) + U_1 c_1 (p(t) - x(t)) + U_2 c_2 (g(t) - x(t)), \tag{3}$$

$$x(t+1) = x(t) + V(t+1), \tag{4}$$

#159136 - $15.00 USD Received 29 Nov 2011; revised 25 Jan 2012; accepted 27 Jan 2012; published 22 Feb 2012

where $U_i\,(i=1,2)$ are independent random uniform variables between 0 and 1, $p(t)$ is the particle best position over previous generations up to step t, $g(t)$ is the global best of $p(t)$, ω is the inertia weight and $c_i\,(i=1,2)$ are the acceleration coefficients. Equation 3 is used to calculate the particle new velocity using its previous velocity and the distances between its current position and its own best $p(t)$ and the global best $g(t)$. Then the particle moves toward a new position following Eq. 4.

The success of PSO strongly depends on values taken by c_1, c_2 and ω. Zhan et al. outlined the necessity of updating these coefficients at each step following the evolutionary state (exploration, exploitation, convergence or jumping out from a local optimum). They estimate the evolutionary state at each step using the previous state and the value of the "evolutionary factor" which is computed using distance between particles. Then based on this estimation, APSO updates the inertia weight and acceleration coefficients. Finally to avoid local optima, APSO performs elitist learning in the convergence state which helps jumping out of the local optima.

The population size is set to 20 as in many PSO studies and in previous work [23]. In that benchmark study, similar problems require 200($\pm$30) evaluations for convergence (results over one thousand realizations). To ensure convergence, the number of evaluations should exceed the maximum reported for similar problems. Therefore a maximum of 300 evaluations is chosen as stop criterion. Furthermore, the convergence state is checked at the end of each loop. Finally, optimizations are repeated twice to confirm the obtained results.

3. Assumptions, results and discussion

3.1. Assumptions and therapeutic cases

The gold nanoparticles should be small enough to penetrate small capillaries and get fixed to cells, typically 10-100 nm or smaller [29, 30]. Therefore we consider nanorods of length within the range 10-100 nm, and nanoshell or hollow nanosphere with maximal inner radius r_1 of 100 nm and maximal shell thickness e of 50 nm (a discussion is held if the optimal size r_1+e exceeds 100 nm). The lower bounds should take account of fabrication control achievement to get realistic and feasible samples. Otherwise, as some improvements of the control in the fabrication process are awaited, the lower bounds can slightly surpass the current fabrication limitations (a discussion is held if the optimal setting does not fit these limitations). The hollow nanospheres can be produced with sizes ranging from 12 nm in outer radius (r_1+e) and 3 nm in shell thickness with a precision of 0.6 nm [7]. Therefore, to be less restrictive, we can consider nanoshells having minimal size parameters of 5 nm for inner radius r_1 and 1 nm for shell thickness e. For small nanorods, the aspect ratio (AR) of fabricated samples are up to six [31]. For flexibility, we choose an aspect ratio between 1 and 8. To sum up, we optimize the size parameters to get the maximal absorption efficiency for the following gold nanoparticles and bounds:

- hollow nanospheres and nanoshells (silica core and gold shell) of radius $r_1 \in [5,100]$ and shell thickness $e \in [1,50]$ (Fig. 2)
- nanorods with the following shapes (as reported in previous studies):
  - spheroids of long diameter D_1 and short diameter D_2 (Fig. 4(a)), where $D_1 \in [10,100]$ nm and the aspect ratio $AR = D_1/D_2 \in [1,8]$
  - cylinders of length L and diameter D (Fig. 4(b)), where $L \in [10,100]$ nm and the aspect ratio $AR = L/D \in [1,8]$
  - cylinders with hemispherical end caps of length (not including caps) L and diameter D (Fig. 4(c)), where $L \in [10,100]$ nm and the aspect ratio $AR = D/(L+D) \in [1,8]$

#159136 - $15.00 USD Received 29 Nov 2011; revised 25 Jan 2012; accepted 27 Jan 2012; published 22 Feb 2012

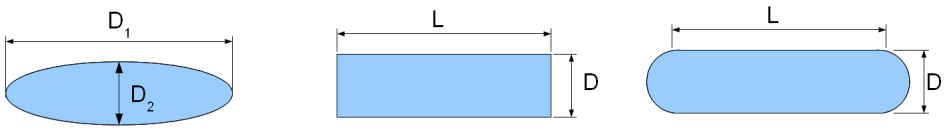

(a) Spheroid (b) Cylinder (c) Capped cylinder

Fig. 4. Different shapes for modeling nanorods.

The choice of the gold optical index may effect the results. This issue was discussed by Ungureanu et al. [32] with comparison to some experiments. However they show dependency on the aspect ratio, and that the optical indexes in classical references are not suitable for all cases. Thus, more detailed comparative studies between theory and experiment should be conducted to resolve this issue. Nevertheless, in a previous sensitivity study on hollow nanospheres, we found that a wide range of wavelengths (difference of 29 nm) ensures 99% of maximal absorption [33]. Therefore the optical index, which depends on wavelength, seems to be a non critical parameter for the maximal absorption and we use the gold optical index of Johnson and Christy [16, 34].

The direction of the linear polarization of light does not influence the level of Q_{abs} for spherical shape because of its symmetry. For the nanorods, on one hand, they are highly sensitive to the polarization along their axis because of their antenna behavior and their plasmonic properties. On the other hand, the nanorods are randomly oriented in cells; therefore a circular polarization is preferred to activate as many nanorods as possible [12]. Consequently, both the circular polarization and linear polarizations are investigated in this study to be closer to therapeutics and to compare with previous results [2, 10, 11].

The diffusion and the depolarization of light in tissue can be another important issue, mainly for medical diagnosis [35]. This parameter would be critical if the power of the incoming light should be determined. However, the computed Q_{abs} is relative to a unity incoming field, which is supposed to be the reference in the vicinity of the nanoparticle embedded in the cells. Therefore the optimization of sizes and shapes does not depend on the depolarization of light. For instance, the nanorods are more sensitive to longitudinal polarization and the contributions of the other polarization would increase Q_{abs} only slightly (Tab. 1).

Finally, regarding the therapeutic cases, we choose to consider the two followings cases:

- **case 1**: treatment of shallow cancer assuming the skin dermis as surrounding tissue (refractive index 1.55 [4]) under illumination $\lambda = 633$ nm (VIS)
- **case 2**: treatment of deep cancer assuming subcutaneous fat as surrounding tissue (refractive index 1.44 [4]) under illumination $\lambda = 800$ nm (NIR)

3.2. Results and discussion

Optimized results

The optimal size parameters, that ensure the maximum absorption efficiency Q_{abs}, are reported in Tab. 1. For optimized nanoshell and hollow nanosphere under linear polarization, and nanorod under circular polarization, the extinction, absorption and scattering efficiency spectra are displayed in Fig.5. As expected, they present maxima for the illumination used for the corresponding therapeutic case.

#159136 - $15.00 USD Received 29 Nov 2011; revised 25 Jan 2012; accepted 27 Jan 2012; published 22 Feb 2012

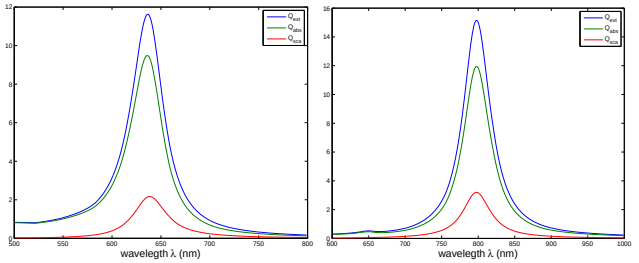

(a) Optimized nanoshell (case 1) (b) Optimized nanoshell (case 2)

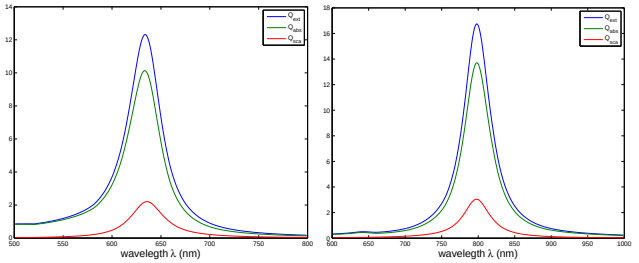

(c) Optimized hollow nanosphere (case 1) (d) Optimized hollow nanosphere (case 2)

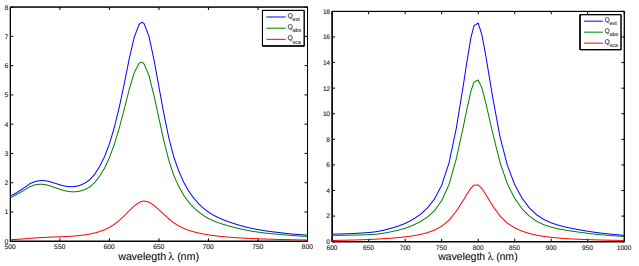

(e) Optimized spheroid (case 1) (f) Optimized spheroid (case 2)

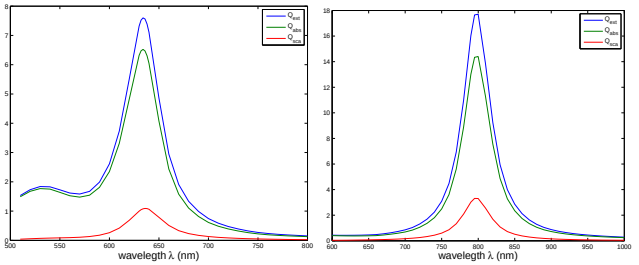

(g) Optimized capped cylinder (case 1) (h) Optimized capped cylinder (case 2)

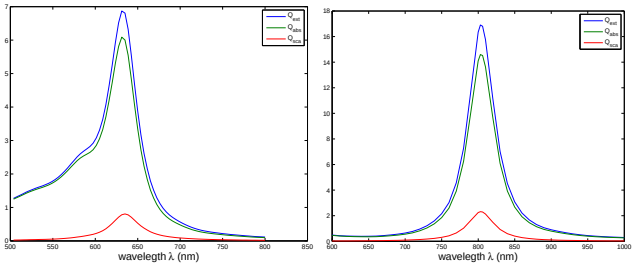

(i) Optimized cylinder (case 1) (j) Optimized cylinder (case 2)

Fig. 5. Extinction (blue curve), absorption (green) and scattering (red) efficiencies for optimized nanoparticles (Mie theory and linear polarization are used to evaluate (a)-(d), and DDA and circular polarization are used for (e)-(j)). The geometrical parameters (Figs. 2 and 4) of each optimized nanoparticle can be found in Tab. 1.

As mentioned previously, the experimental studies are limited to some manufactured samples which may prevent finding the most absorbant ones for a particular therapy case. Therefore the purpose of such studies was always to find among all the studied samples, the one whose maximum absorption efficiency matches with the target laser wavelength. Numerous samples can fit this condition but without ensuring the maximum absorption. Comparing our results with the previous theoretical studies where no optimization tools were used, the optimization tools yield better results. To illustrate:

- A maximal Q_{abs} of 6 for nanoshell in the study by Vera and Bayazitoglu [36] (that study takes into account different optical indexes of tissue but nanoshell size was fixed independently) v.s. Q_{abs} greater than 9 in this paper.
- An extinction efficiency not exceeding 8 for different shapes of nanorods, optical indexes of gold and wavelengths, in the theoretical part of the study carried by Ungureanu et al. [32], whereas we find Q_{ext} up to 17 as it could be seen in Fig. 5 (we should note that both studies use DDA).
- An absorption efficiency not exceeding 8 in the theoretical study by Lee and El-Sayed [16] that considers different shapes for nanorods, whereas Q_{abs} reaches 14 as reported in Tab. 1.

Table 1. Optimized shape parameters (Figs. 2 and 4) of gold nanoparticles in the two therapeutic cases: case 1, the nanoparticles are embedded in skin dermis, using 633 nm illumination wavelength; case 2, the nanoparticles are embedded in subcutaneous fat, using 800 nm illumination wavelength. [a]: DDA is used to evaluate Q_{abs}; [b]: the full Mie theory and linear polarization are used to evaluate Q_{abs}.

Shape		λ=633 nm		λ=800 nm	
		Parallel polarization	Circular polarization	Parallel polarization	Circular polarization
Spheroid [a]	D_1 (nm)	51	52	74	79
	D_2 (nm)	28	29	22	24
	Q_{abs}	12.6	6.3	25.4	12.6
Capped cylinder [a]	L (nm)	19	18	42	44
	D (nm)	26	24	19	19
	Q_{abs}	12.9	6.6	27.7	14.4
Cylinder [a]	L (nm)	30	30	49	49
	D (nm)	24	24	18	17
	Q_{abs}	12.2	6.4	28.1	14.2
Nanoshell [b]	r_1 (nm)	14		22	
	e (nm)	6		3.5	
	Q_{abs}	9.2		11.8	
Hollow nanosphere [b]	r_1 (nm)	14		20	
	e (nm)	5		2.5	
	Q_{abs}	10.1		13.6	

Nanoshell v.s. hollow nanosphere

For both the therapeutic cases, the optimized hollow nanospheres are slightly smaller than the optimized nanoshells (silica core coated with gold) and exhibit higher absorption efficiency (Tab. 1). The improvement is by 11% in the first therapeutic case and by 14 % in the second

#159136 - $15.00 USD Received 29 Nov 2011; revised 25 Jan 2012; accepted 27 Jan 2012; published 22 Feb 2012

one. This improvement may be considered slight however, the hollow nanosphere should be preferred, especially as getting a uniform shell on the silica core remains challenging [2, 37].

Choice of nanorod shape

Lee and El-Sayed [16] suggested that capped cylinder would better describe nanorods. However Ungureanu et al. [32] found that, in some cases, ellipsoids or cylinders have spectral extinction closer to experiments. On the other side, when comparing the optimized three shapes, we find that in two cases, the optimized spheroid, capped cylinder and cylinder have different total length (D_1 for spheroid, $D+L$ for capped cylinder and L for cylinder). However they have similar absorption efficiencies (difference less than 13%). Therefore we suggest for each therapeutic case, the fabrication of optimized samples with the optimal length and width (Tab. 1) and the measurement of their spectra to check the theoretical results (Fig. 5).

Effect of polarization on optimal setting of nanorod

The results reported in Tab. 1 show that the maximum absorption efficiency depends on the polarization. However the size parameters seem to hardly depend on this parameter (almost the same optimal size parameters for spheroid, capped cylinder and cylinder). In fact, the circular polarization should be able to excite almost all plasmon oscillation modes including the longitudinal one. The longitudinal mode (which appears when using parallel polarization) presents the most important absorption efficiency, therefore its contribution to Q_{abs} when using circular polarization should be the most important. Then, the most absorbing structure, illuminated with a linear polarization, is likely to do as well when illuminated with circular polarization. The efficiency of linear polarization, is nearly twice that of circular polarization. This comes from the equal distribution of the energy of the incoming electric field, on the two perpendicular directions, for the circular polarization. This confirms the relevance of the heuristic reasoning made above.

Hollow nanosphere v.s. nanorod and influence of the Full Width at Half Maximum (FWHM) of the illumination

In each therapeutic case, the comparison between the optimized hollow nanosphere (linear polarization) and nanorod (circular polarization) can be based on the three following criteria: the absorption efficiency Q_{abs}, the narrowness of the absorption band and gold volume. The results reported in Tab. 1, show that the optimized hollow nanosphere is more absorbent than the optimized nanorod in the VIS therapy case (633 nm and skin dermis as surrounding tissue). Both nanoparticles have almost similar behavior in the NIR therapy case (for the different possible shapes of nanorods). Thus, nanorods are not the most efficient nanoparticles for PTT. Regarding the absorption band, its narrowness enables a better match with the laser illumination and prevent the patient sensitivity to the parasite light. Figure 6 shows that the optimized nanorod has also a narrow absorption band, comparable to that of the hollow nanosphere, in the NIR. However its absorption band presents a second resonance in the VIS. Finally, the hollow nanospheres are small enough for their injection in tissue but are larger than nanorods (Tab. 1). The gold volume of the optimized hollow nanosphere, that may be crucial for the manufacturing cost, is 17×10^3 nm^3 which is less than the optimized spheroid volume (similar results are obtained in the second therapeutic case: the gold part is approximatively 14×10^3 nm^3 v.s. 24×10^3 for spheroid, 16×10^3 nm^3 for capped cylinder and 13×10^3 nm^3 for cylinder).

Hollow nanosphere and nanorod have similar efficiencies in therapeutic case 2. Therefore the influence of the FWHM of the illumination deserves to be studied to depict its impact on their efficiency. For this, the wavelength is varied within the quarter of the bandwidth i.e. 800+/-25 nm for both the hollow nanosphere and the capped cylinder in therapeutic case 2, as illustration. Their maximal absorption efficiencies are shown in Fig. 7.

The maximal absorption efficiency of nanorods increases of less than 10% as the wavelength increases, showing that a higher wavelength ensures higher efficiency of optimized nanorods.

#159136 - $15.00 USD Received 29 Nov 2011; revised 25 Jan 2012; accepted 27 Jan 2012; published 22 Feb 2012

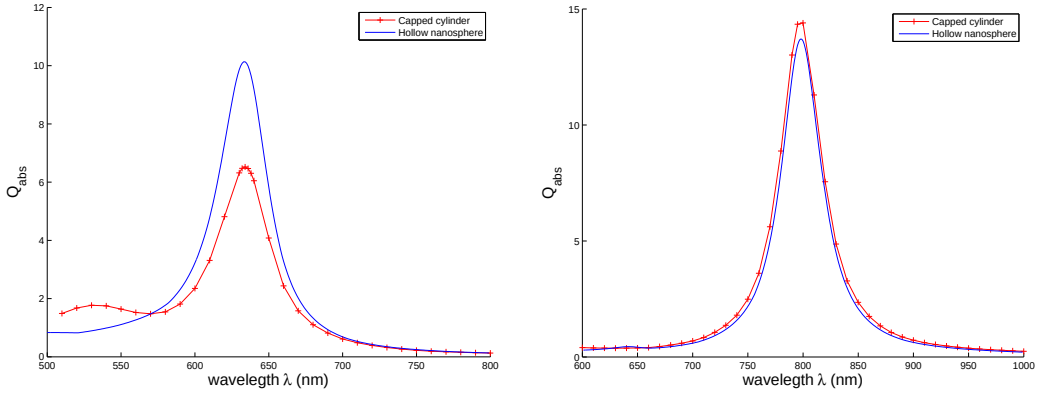

(a) in the VIS range (therapy case 1)

(b) in the NIR range (therapy case 2)

Fig. 6. Comparison of the absorption band of optimized capped cylinder and hollow nanosphere (Tab. 1), DDA is used to get the spectra of capped cylinder and Mie theory is used to get spectra of hollow nanosphere.

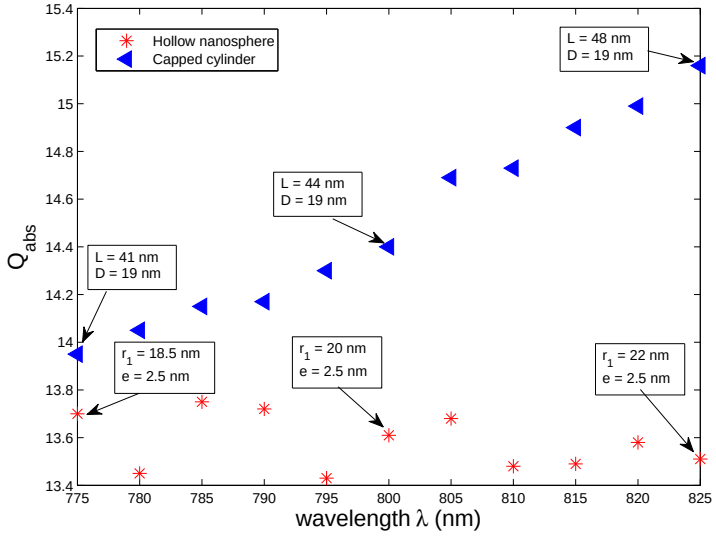

Fig. 7. Maximal absorption efficiencies of hollow nanosphere and nanorod for wavelengths within the quarter of the bandwidth of the illumination *i.e.* 800 ± 25 nm.

However the hollow nanosphere presents only slight fluctuations of the maximal absorption efficiency. Given the values of absorption efficiency over the range of wavelengths, all of the optimized nanoparticles can be considered active (Fig. 7).

Within this range of wavelengths, slight variations are observed on optimal size parameters of both nanoparticles. The gold shell thickness e of the optimized hollow nanosphere remains equal to 2.5 nm (Tab. 1) over the whole range of wavelengths, and the inner radius r_1 is between 18.5 to 22 nm. Despite the capped cylinder is more sensitive to the wavelength, its optimal diameter D remains equal to 19 nm over the range of wavelengths and only its length L increases

#159136 - $15.00 USD Received 29 Nov 2011; revised 25 Jan 2012; accepted 27 Jan 2012; published 22 Feb 2012

from 41 nm to 48 nm. Consequently, the critical parameters are e for the hollow nanosphere, and D for the capped cylinder. The improvement of the fabrication process should be focused on a better control of these parameters; otherwise, the efficiency of nanoparticles could drop. These first results confirm those obtained in Ref. [13], but deserve to be expanded through a study of design tolerance.

Design tolerance for the size parameters

The probability laws governing the uncertainties are neither identified nor quantified experimentally, hence a study of the propagation of uncertainty may be hazardous. On the other hand, the tolerance analysis helps to deduce the critical parameters, on which effort to control the fabrication should be made. This approach consists of considering an acceptable threshold of the efficiency, and deducing the corresponding tolerance for the size parameters [34]. Above this threshold, the nanoparticles are considered as active for the therapy. The activity of the nanoparticles depends on both the incoming illumination properties and those of the tissue. Nevertheless, the arbitrary choice of the threshold enables to quantify the relative tolerances for each geometrical parameter.

The best nanoparticles found are subjected to this analysis i.e. the hollow nanosphere for the two therapeutic cases and all the nanorod shapes for the second therapeutic case. To carry this study, either the method described in [34], or a direct local search can be used. We consider a threshold of 90% of the maximal absorption efficiency for each nanoparticle, and report results in Tab. 2 as well as Fig. 8.

Table 2. Design tolerance for the size parameters (min-max values) for a threshold 90% of maximal absorption efficiency (obtained from the optimum setting of the size parameters) in both therapeutic cases.

Shape	Size parameters	Minimum	Maximum
Spheroid	D_1 (nm)	60	93
in therapy case 2	D_2 (nm)	17	28
	aspect ratio AR	3.3	3.5
Capped cylinder	$L+D$ (nm)	47	76
in therapy case 2	D (nm)	14	24
	aspect ratio AR	3.1	3.4
Cylinder	L (nm)	41	66
in therapy case 2	D (nm)	14	24
	aspect ratio AR	2.7	3.0
Hollow nanosphere	e (nm)	3.4	6.8
in therapy case 1	r_1 (nm)	10.2	17.8
	e/r_1	2.6	3.0
Hollow nanosphere	e (nm)	1.8	3.2
in therapy case 2	r_1 (nm)	14.8	25.1
	e/r_1	7.7	8.4

The tolerance is ± 1.7 nm for e and ± 3.8 nm for r_1 in therapeutic case 1 (resp. ± 0.7 nm and ± 5.1 nm in case 2), for the hollow nanospheres. These tolerances can be respected, given the current fabrication precision of 0.6 nm [7], even if the "golden rule" of metrology is more restrictive on the maximal uncertainties in the fabrication process. However, as demonstrated in a previous work [34], more attention should be devoted to the coating design e as the tolerance for this parameter is lower than the tolerance for r_1. Moreover, the ratio r_1/e should be within a specific range as reported in Tab. 2 and illustrated by the seemingly-linear dependance between e and r_1 in Fig. 8.

#159136 - $15.00 USD Received 29 Nov 2011; revised 25 Jan 2012; accepted 27 Jan 2012; published 22 Feb 2012

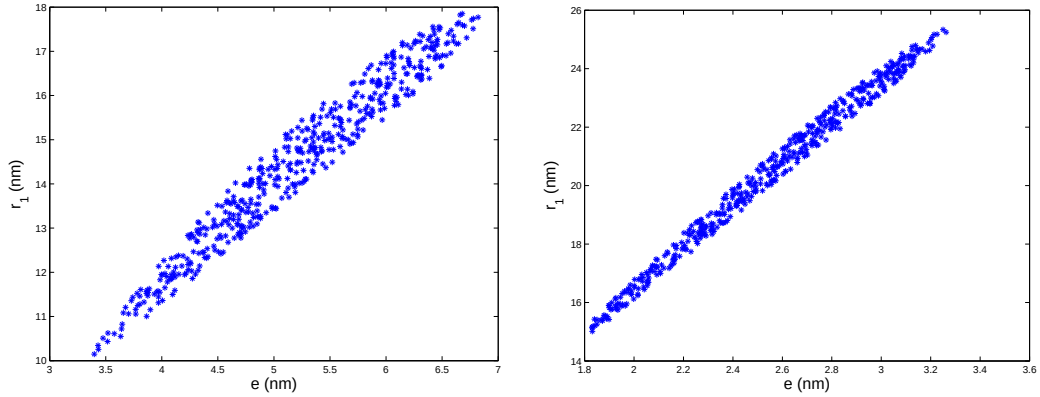

(a) therapy case 1 (b) therapy case 2

Fig. 8. Size parameters (shell thickness e and inner radius r_1) of hollow nanosphere ensuring 90% of maximal absorption efficiency of hollow nanosphere in therapeutic case 1 (nanoparticles injected in skin dermis and illuminated by a 633 nm laser) and case 2 (nanoparticles injected in subcutaneous fat and illuminated by a 800 nm laser).

Regarding the different shapes of nanorods, results show a tolerance for length of about ± 15 nm and a tolerance for width of about ± 5 nm (Tab. 2). For the both size parameters, the relative tolerance falls between 21% and 26%. The proposed samples of nanorods (with tolerances) can be synthesized successfully as the fabrication precisions are less than 5 nm [38, 39]. Nevertheless, to increase the ratio of active nanoparticles, and therefore to decrease their concentration while maintaining constant the therapeutic efficiency, the uncertainties on their geometrical parameters should be decreased. The relative tolerance for the aspect ratio (AR) is much more restrictive ($\leq 5.3\%$). Therefore, the nanorods can have different lengths (what is usually obtained after synthesis) but should have a given aspect ratio, for a given therapy case.

4. Conclusions

To get the maximum absorption efficiency in two therapeutic cases, the theoretical optimization of the size parameters of silica-gold nanoshells, hollow nanospheres and nanorods was carried out. The optimization of the absorption efficiency (computed with either the full Mie theory or the discrete dipole approximation) is achieved by an adequate Particle Swarm Optimization algorithm. The results show an improved efficiency compared with previous studies. The optimized hollow nanospheres are slightly smaller and more efficient than the optimized nanoshells. Absorption band of nanorods and hollow nanospheres have similar shape and narrowness in the infrared therapy case. It is also shown that under circular polarization, which is recommended in practice, the optimized hollow nanospheres could be more efficient than the nanorods. This is the opposite of the commonly reported results assuming polarization parallel to the longitudinal axis of the nanorod. The influence of the polarization and of the FWMH of the illumination is also analyzed. Finally a design tolerance analysis for the size parameters, reveals that the current fabrication precision is sufficient to guarantee 90% of maximal absorption efficiency.

For further applications (other laser wavelengths, tissue of different optical indexes, or both), the same numerical tools can be used to find the optimal parametric setting. It could be interesting to produce the optimized samples suggested in this study mainly to identify which shape

#159136 - $15.00 USD Received 29 Nov 2011; revised 25 Jan 2012; accepted 27 Jan 2012; published 22 Feb 2012

better describes the real nanorods. Experiments could also help to recover the true optical index of gold nanoparticles, depending on the process of fabrication.

Acknowledgments

Authors thank the Région Champagne-Ardennes, the Conseil Régional de l'Aube and the *Nanoantenna* European Project (FP7 Health-F5-2009-241818) for financial supports.

#159136 - $15.00 USD Received 29 Nov 2011; revised 25 Jan 2012; accepted 27 Jan 2012; published 22 Feb 2012